Stability of anhydrous phase B: Experimental studies and implications for phase relations in subducting slab and the X discontinuity in the mantle

Jibamitra Ganguly[1] and Daniel J. Frost[2]

[1]   We have experimentally determined the equilibrium boundary of the reaction forsterite (Fo) + periclase (Per) = anhydrous phase B (Anh-B) at $900°-1600°C$, and we used the retrieved Gibbs free energy of formation of Anh-B to calculate the stability field of Anh-B + stishovite (Sti) with respect to the Mg_2SiO_4 polymorphs. The results suggest the possibility of the reaction sequence wadsleytite $\rightarrow$ Anh-B + Sti $\rightarrow$ ringwoodite with increasing pressure at temperature below $\sim600°C$. This might lead to an eye-shaped splitting of the 410 km discontinuity within the interior of a sufficiently cold slab, such as would prevail in a 140 Myr old slab subducting at an angle of $\sim60°$ with a rate of ≥ 14 cm/yr (e.g., Tonga). The equilibrium boundary of Anh-B + Sti with respect to the wadsleyite and ringwoodite has, respectively, positive and negative slope in the P-T space. The reaction of Fo + Per to Anh-B seems to offer a viable explanation of the so-called X discontinuity that has been observed at $275-345$ km depth in several subcontinental and subduction zone environments. It is suggested that periclase could form locally by the dissolution of silica in mantle fluid or precipitate from a hydrous melt that became enriched in MgO due to the incongruent melting of olivine at pressures of $6-8$ GPa.

Citation: Ganguly, J., and D. J. Frost (2006), Stability of anhydrous phase B: Experimental studies and implications for phase relations in subducting slab and the X discontinuity in the mantle, *J. Geophys. Res.*, *111*, B06203, doi:10.1029/2005JB003910.

1.   Introduction

[2]   Anhydrous phase B (Anh-B) is a dense anhydrous magnesian silicate with the Mg end-member stoichiometry of $Mg_{14}Si_5O_{24}$. It was first synthesized by *Herzberg and Gasparik* [1989]. *Finger et al.* [1991] solved the crystal structure of this mineral and showed that it consists of two types of layers. One is a rock salt type layer with edge-shared Mg and Si octahedra, and the other a forsterite type layer with Mg octahedra and Si tetrahedra. Phase B, which has structural water with the stoichiometry $Mg_{12}Si_4O_{19}(OH)_2$, has a similar structural configuration with the forsterite type layers replaced by layers with the stoichiometry of humite. There are six layers per unit cell, in which each octahedral layer is flanked by two tetrahedral layers.

[3]   It is generally accepted that with increasing pressure in the Earth's mantle, Mg-rich olivine (α) undergoes the transformation $\alpha \rightarrow \beta$ (wadsleyite: Wads) $\rightarrow \gamma$-spinel (ringwoodite: Rng). The olivine $\rightarrow$ Wads and Wads $\rightarrow$ Rng transformations are believed to be the reason for the observed seismic discontinuities at ~410 and 520 km depths. However, Mg_2SiO_4 could, in principle, transform to Anh-B plus stishovite (SiO_2) or ilmenite ($MgSiO_3$) under certain P-T conditions. In addition, olivine could react with MgO (periclase: Per) in a relatively silica deficient portion of the mantle to form Anh-B. The formation of Anh-B by these reactions within the Earth's mantle and subducting slab could have important seismic consequences, and also might alter the density structure of a subducting slab thus modifying the slab-pull force of plate subduction.

[4]   A preliminary study of the possible stability limit of the hydrous phase B was reported by *Kato and Kumazawa* [1985]. The stability limit was approximately defined on the basis of the results of synthesis experiments starting with a mixture of periclase and forsterite in a multianvil apparatus, but without shielding the starting mixture from reacting with water that is typically given off from the dehydration of the pressure medium (sintered magnesia). Electron microprobe analysis of the reaction product of For + Per + water yielded Mg/Si ≈ 2.9. *Herzberg and Gasparik* [1989] argued that the Mg/Si reported by Kato and Kumazawa was almost identical to what they found (Mg/Si = 3) for a similar phase that was produced in melting experiments on chondrite, in which special care was taken to keep the sample under anhydrous condition. This would imply that *Kato and Kumazawa* [1985] investigated the stability of Anh-B instead of B. However, subsequent study by *Finger et al.* [1991] shows that it is the hydrous phase, B, and not Anh-B that has an Mg/Si ratio of 3. According to their results, the Mg/Si ratio of Anh-B in the system Mg-Si-O system is 2.8. Thus we conclude that the stability of the phase investigated by *Kato and Kumazawa* [1985] was most likely that of the hydrous phase, B. Also, inasmuch as *Finger et al.* [1991] obtained their sample of Anh-B from the experiments of

---

[1]Department of Geosciences, University of Arizona, Tucson, Arizona, USA.
[2]Bayerisches Geoinstitut, Universität Bayreuth, Bayreuth, Germany.

Herzberg and Gasparik [1989], it seems that the Mg/Si ratio reported by the latter for their experimental product was erroneous.

[5] In this work, we have determined the equilibrium boundary of the reaction Fo + Per = Anh-B by "reversed" phase equilibrium experiments. In addition, the thermochemical properties of Anh-B retrieved from this boundary and estimated by empirical methods were used to explore the likely P-T conditions for the transformation of wadsleyite and ringwoodite to Anh-B plus stishovite. The low temperature and the consequent sluggish reaction kinetics hinder direct experimental study of this reaction. Finally, we show that the transformation of Fo + Per to Anh-B is likely to be at least partly responsible for the seismic discontinuity at ∼300 km depth that has been observed in several parts of the Earth's mantle.

2. Experimental Procedure

[6] Anh-B was presynthesized for the phase equilibria experiments from encapsulated (see below) stoichiometric oxide mixtures of MgO and SiO_2 in a multianvil apparatus at 10 GPa, 1200°C. Electron microprobe analysis of a synthetic product yielded Mg/Si ratio of 2.78 ± 0.02 (2σ) for the average of 19 spot analyses. This composition is in excellent agreement with that reported by *Finger et al.* [1991] for the Anh-B sample that was used in their crystallographic studies. A mixture of either synthetic Anh-B, synthetic forsterite and synthetic periclase, or simply of forsterite plus periclase, was tightly packed inside a cylindrical Mo capsule of ∼1.5 mm length and 1.6 mm diameter. The capsules were closed at both ends by hammering within a close fitting die, and were loaded into 14 mm edge length octahedral pressure cells that employed $LaCrO_3$ internal resistance furnaces. The furnace had a stepped design in order to reduce the temperature gradient along the length of the sample capsule. For further details of the sample assembly, see *Keppler and Frost* [2005]. The sample assembly was dried for ∼24 hours in a vacuum furnace and then compressed in a multianvil device using tungsten carbide cubes with 8 mm edge length corner truncations. Run durations varied from 1 to 5 hours depending on the temperature. Temperature was monitored during the experiment using a $W_{97}Re_3$-$W_{75}Re_{25}$ thermocouple with the junction positioned just above the sample capsule. The pressure was calibrated between 9 and 14 GPa using the SiO_2 coesite-stishovite transformation at 1200°C and the Mg_2SiO_4 forsterite-wadsleyite transformation at 1000°C, as reported by *Keppler and Frost* [2005]. The uncertainty arising from the fitting of the calibration curve and from the published experimental data used in the calibration is approximately 0.5 GPa. No correction for the pressure effect on the thermocouple EMF was applied. Because of thermal gradient in the pressure cell, the mean temperature of a sample could have differed by ±25°C from the nominal temperature recorded by the thermocouple, as suggested by our earlier studies on the thermal gradients in similar pressure cells using Mo capsules.

[7] The choice of the P-T conditions for the experiments was guided by thermodynamic analysis of the possible equilibrium condition of the reaction of Fo and Per to form Anh-B, using the available thermodynamic properties of Fo and Per and the estimated properties of Anh-B, as discussed in the next section. After completion of the experiment, the sample was quenched, recovered from the pressure cell assembly, and examined by powder X-ray diffraction and, occasionally, by micro-Raman spectroscopy. The change in the relative intensities of selected X-ray reflections from those in the starting mixture was used to monitor the direction of the reaction.

3. Determination of the Equilibrium Boundary Between Fo + Per and Anh-B

[8] In a chemically balanced form, the reaction of Fo plus Per to Anh-B is written as

(R1)   5Fo + 4 Per = Anh-B

Since there were no data to lead us to a restricted P-T domain in which to search for the equilibrium boundary for the experimental studies, we tried to roughly estimate the boundary from the available and inferred thermochemical data of the minerals. We outline this procedure here as it may be useful in guiding initial experiments in similar high-pressure phase equilibria studies.

[9] The Gibbs free energy (in short, Gibbs energy) of formation from the elements, $\Delta_f G$, of Anh-B was estimated according to following scheme:

$$\Delta_f G(\text{Anh-B}) = 5[\Delta_f G(\text{Fo})] + 4[\Delta_f G(\text{Per})] \\ + [\Delta_f G(\text{Sti}) - \Delta_f G(\text{Qtz})] \qquad (1)$$

The rationale for this scheme lies in the success of the polyhedral approach for the estimation of thermochemical properties [*Chermak and Rimstidt*, 1989]. The last term within the square bracket is intended to account for the effect of coordination change of one silicon atom from four to six.

[10] Throughout this paper, we have used the computerized version (S. K. Saxena, personal communication, 2005) of the thermochemical database developed by *Fabrichnaya et al.* [2004] for high pressure calculations as these data used well behaved PVT relations and C_P functions that satisfy theoretical constraints at high P-T conditions. From these data, (1) yields −12,271 kJ/mol for $\Delta_f G$ (Anh-B) at 10 kbar, 1300 K. Using the Gibbs energy and volume data for Fo and Per at 10 kbar, 1300 K from *Fabrichnaya et al.* [2004] and V(Anh-B) from *Finger et al.* [1991], and assuming that the ΔV of the reaction (R1) is independent of the change of P-T condition along the equilibrium boundary, we obtain an equilibrium pressure of 8.35 GPa at 1300 K for the above reaction (Figure 1), using standard thermodynamic procedure [e.g., *Ganguly and Saxena*, 1987, equation F.3, chapter 4].

[11] With the above initial estimate of a possible equilibrium condition of Anh-B we focused on experiments to constrain the equilibrium condition at 900°–1000°C by determining the conditions of growth of Anh-B from Fo + Per and the reverse reaction. The experimental data, which are illustrated in Figure 1, yield an equilibrium pressure of ∼10.2 GPa at 1027°C, which is ∼1.85 GPa higher than the crude estimate of the equilibrium pressure at the same
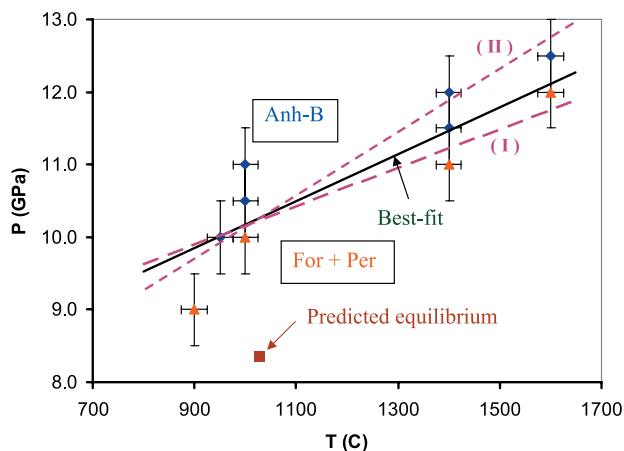
Figure 1. Stability of anhydrous B (Anh-B) with respect to forsterite (Fo) plus periclase (Per). The experimental data are indicated by symbols with error bars. Triangles indicate formation of Fo + Per from Anh-B; diamonds indicate reverse reaction. The solid square indicates the equilibrium pressure at 1300 K, as estimated using polyhedral thermochemical properties of Anh-B. The dashed lines indicate estimated P-T slopes using $\Delta_r V$ and $\Delta_r S$ data at 1 bar, 298 K (curve I) and 10 GPa, 1300 K (curve II) (see text).

temperature. After these initial experiments, we delineated a range of P-T slope to guide our experimental studies to constrain the equilibrium boundary at different conditions.

[12] In the experiment at 10 GPa, 1000°C, for 5 hours (run H-1807, Table 1) using a starting mixture of Anh-B + Fo + Per, we found Anh-B only at the bottom of the capsule after quenching the experiment. This observation was interpreted to be due to the difference of temperature (ΔT) between the top and bottom of the capsule that spanned across the equilibrium boundary between Fo + Per and Anh-B. From our earlier measurements of temperature gradient, we estimated ΔT to be ~50°C. Thus the temperature at the top of the capsule, which is the measured temperature of 1000°C, is shown to be in the field of Fo + Per, whereas the estimated temperature of 950°C at the bottom of the capsule is shown to be in the field of Anh-B. We found from other experiments at 900 and 1000°C that a run duration of 5 hours was enough for complete reaction.

[13] In the absence of any entropy datum for Anh-B that is needed to calculate the P-T slope of equilibrium (R2), we estimated it as follows:

$$S(\text{Anh-B}) = \sum S(\text{oxides}) + \Delta S(\text{volume effect})$$
$$+ \Delta S(\text{coordination effect}), \quad (2)$$

where the first term on the right indicates the sum of the entropies of the component oxides, the second term accounts for the effect of volume change in the formation of Anh-B from the component oxides, and the third term accounts for the change in the coordination number of one silicon from tetrahedral in the oxide to octahedral in Anh-B. The volume effect term was estimated according to the method of *Holland* [1989], which was modified from *Fyfe et al.* [1958]. For the effect of change of coordination number of Si, we used the entropy change of the reaction $^{[4]}SiO_2$ (quartz) $\rightarrow$ $^{[6]}SiO_2$ (stishovite), where the left-hand superscript indicates the coordination number. This procedure yields a third law entropy of Anh-B at 1 bar, 298 K to be 547.3 J/mol K. The entropy and volume data for the oxides required for this calculation are from *Saxena et al.* [1993].

[14] Using the above entropy estimate for Anh-B and the entropy and volume data for Fo and Per from *Saxena et al.* [1993] and V(Anh-B) from *Finger et al.* [1991], we have calculated the P-T slope of the equilibrium boundary for the reaction (R1) at 1 bar, 298 K according to the well known relation dP/dT = $\Delta S/\Delta V$, where ΔS and ΔV denote, respectively, the entropy and volume change of a reaction. Thus we obtained dP/dT = 26.7 bar/K. An equilibrium boundary satisfying this slope and the experimental data at 950°–1000°C is illustrated in Figure 1 as curve I.

[15] An alternative estimate of the P-T slope of the reaction boundary was carried out by considering the possible P-T dependence of ΔS and ΔV of the reaction. The V and S of Anh-B at high P-T condition were estimated from the data at 1 bar, 298 K, assuming, in the spirit of the "polyhedral model" (1), that the changes of these properties with the change of P-T condition can be approximated according to

$$dY(\text{Anh-B}) = 5dY(\text{Fo}) + 4dY(\text{Per}) + [dY(\text{Sti}) - dY(\text{Qtz})] \quad (3)$$

where Y is either V or S. This procedure led to dP/dT = 45.3 bar/K at 10 GPa, 1300 K. This slope is illustrated as

Table 1. Summary of Experimental Data for the Determination of the Equilibrium Fo + Per = Anh-B[a]

Run	Starting Material	P, GPa	T, °C	Time, hours	Result
H-1778	1	12.0	1400	4	Anh-B, complete reaction
H-1788	2	11.0	1400	4	growth of Anh-B
H-1791	2	11.0	1000	5	Anh-B, complete reaction
H-1795	2	10.5	1000	5	Anh-B, complete reaction
H-1801	2	11.5	1400	2	growth of Anh-B
H-1780	1	9.0	900	4	Fo + Per, complete reaction
H-1807	2	10.0	1000	5	Fo + Per and small amount of Anh-B at the bottom
H-1886	1	12.0	1600	2.5	Fo + Per
H-1893	1	12.5	1600	2.5	Fo + Per and small amount of Anh-B + Per
H-2063	1	12.5	1600	3	Anh-B + Per

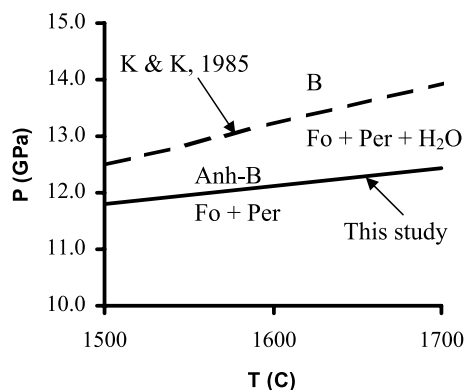[a]Starting materials are 1, Fo + Per; and 2, Anh-B + Fo + Per.

Figure 2. Comparison between the stabilities of hydrous B, as determined by *Kato and Kumazawa* [1985] on the basis of syntheses experiments, and anhydrous B, as determined in this study. The solid line shows the "best fit" line from Figure 1.

curve II in Figure 1, constraining it to satisfy the equilibrium data at 950–1000°C.

[16] With the above estimates for the probable location of the equilibrium boundary of reaction (R1), we carried out additional experiments to constrain the boundary at 1400 and 1600°C. The results are illustrated in Figure 1 along with a "best fit" boundary constrained by all experimental data. It is satisfying to note that this boundary lies between the predicted boundaries. The experimental data seem to be in somewhat better agreement with the predicted boundary (curve I), which was calculated by assuming that the ratio $\Delta S/\Delta V$ along the equilibrium boundary at the high P-T condition is the same as that calculated at 1 bar, 298 K.

[17] Figure 2 shows a comparison between the Fo + Per = Anh-B equilibrium, as determined in this work, and the reaction boundary Fo + Per + H_2O = B that was suggested by *Kato and Kumazawa* [1985] on the basis of syntheses experiments. Since the field of thermodynamic stability of a set of phases cannot be larger than that of any of its subsets, the reaction boundary suggested by *Kato and Kumazawa* [1985] cannot represent a true stability limit of Fo + Per + H_2O; it is a metastable boundary at best. However, as the pressure calibration of *Kato and Kumazawa* [1985] was only performed at room temperature, it is quite possible that they over estimated the sample pressures in their experiments.

4. Calculation of the Boundaries Mg_2SiO_4 (Fo/Wads/Rng) = Anh-B + Stishovite

[18] The "best fit" equilibrium boundary for (R1) defines an equilibrium pressure of 10.1 GPa at 1300 K. Using $\Delta_f G$ values of Fo and Per from *Fabrichnaya et al.* [2004], and the relation $\Delta_r G(10.1 \text{ GPa}, 1300 \text{ K}) = 0 = \Delta_f G(\text{Anh-B}: 10.1 \text{ GPa}, 1300 \text{ K}) - 5\Delta_f G(\text{Fo}: 10.1 \text{ GPa}, 1300 \text{ K}) - 4\Delta_f G(\text{Per}: 10.1 \text{ GPa}, 1300 \text{ K})$, we obtain

$$\Delta_f G(\text{Anh-B}: 10.1 \text{ GPa}, 1300 \text{ K}) = -12{,}237 \text{ kJ/mol}, \quad (4)$$

There is an uncertainty of ~0.4 GPa in the location of the equilibrium boundary (R1) at 1300 K, which leads to an uncertainty of $\sim \pm 100$ kJ in the retrieved value $\Delta_f G$ of

Anh-B at 10.1 GPa, 1300 K. Although this is only ~1% of the best fit value of $\Delta_f G$ of Anh-B, its effect is too large for any meaningful phase equilibrium calculation. The value of $\Delta_f G(\text{Anh-B})$ at 10.1 GPa, 1300 K, as estimated according to (1), is −12,256 kJ/mol. Thus we assume that the value of $\Delta_f G$ of Anh-B in (4) is probably not too far from its true value, and use it to calculate a few other equilibria of potential interest for the mineralogical properties of relatively cold subducting slabs.

[19] The experimentally constrained value of $\Delta_f G(10.1 \text{ GPa}, 1300 \text{ K})$ of anhydrous B, as given in (4), along with the $\Delta_f G$ for forsterite, wadsleyite, ringwoodite and stishovite [*Fabrichnaya et al.*, 2004], were used to calculate the Gibbs energy change, $\Delta_r G$, of the following reactions:

(R2)   Anh-B + 2 Sti = 7 Rng

(R3)   Anh-B + 2 Sti = 7 Wads

(R4)   Anh-B + 2 Sti = 7 Fo

At 10.1 GPa, 1300 K, we obtained $\Delta_r G_{(R2)} = 17.254$ kJ/mol, $\Delta_r G_{(R3)} = -30.129$ kJ/mol, and $\Delta_r G_{(R4)} = -74.208$ kJ/mol. The equilibrium pressure, P_e, at 1300 K for the above reactions can now be calculated according to

$$\Delta_r G(P_e, T) = 0 = \Delta_r G(P', T) + \int_{P'}^{P_e} \Delta_r V dP \quad (5)$$

where $P' = 10.1$ GPa and T = 1300 K. This equation was solved for P_e at 1300 K in two different ways, as discussed below.

[20] On the basis of the successful prediction of the P-T slope of reaction (R1) using $\Delta_r V$ and $\Delta_r S$ data at 1 bar, 298 K, we assume that the $\Delta_r V$ values of the equilibria (R2), (R3) and (R4) at the high P-T condition could also be approximated by $\Delta_r V(1 \text{ bar}, 298 \text{ K})$, and thus solved for P_e at 1300 K for these equilibria. Next, by imposing the P-T slopes of the respective equilibria, as calculated from the 1 bar, 298 K values of $\Delta_r S$ and $\Delta_r V$, we obtained approximate P-T boundaries delineating the condition of formation of Anh-B + Sti from Mg_2SiO_4 (Fo/Wads/Rng) according to the equilibria (R2), (R3) and (R4), respectively. The calculated P-T conditions are illustrated in Figure 3 along with the experimentally determined P-T location of 5 Fo + 4 Per = Anh-B, and the P-T conditions for the transitions Fo → Wads → Rng, as calculated by *Saxena* [1996] from optimized thermodynamic database [*Saxena et al.*, 1993]. The locations of the equilibria have been slightly adjusted (within 0.5 GPa) to satisfy the mutual compatibility relations in that the intersection of the equilibria (R2) and (R3) must lie on the Wads ↔ Rng boundary and that between (R3) and (R4) must lie on the Fo ↔ Wads boundary. The equilibrium (R4) has a slightly more positive slope than that of the Fo to Wads transition, and is thus not shown in Figure 3.

[21] We also show in Figure 3 the effect of lowering the $\Delta_f G$ of Anh-B by 5 kJ/mol (or 0.04%) from the experimentally constrained value of −12,237 kJ/mol. It causes signif-
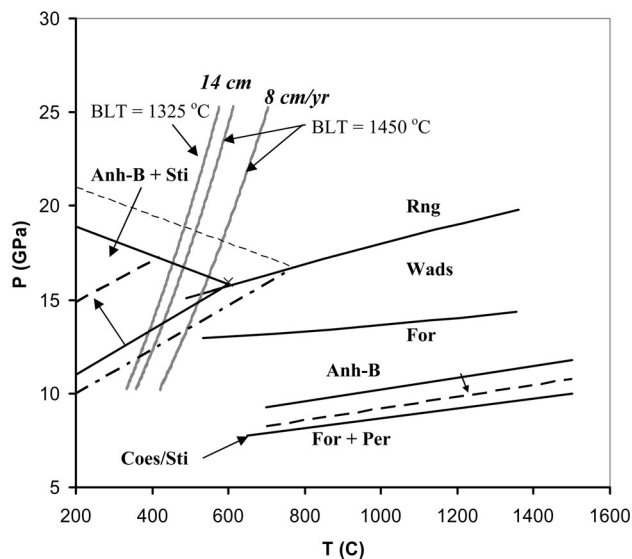
Figure 3. Experimentally determined and calculated stability limits of Anh-B ± Stishovite (Sti) along with the equilibrium boundaries for coesite–stishovite transition and polymorphic transformations of Mg_2SiO_4 (For/Wads/Rng). The effect of solid solution in the anhydrous system on Anh-B + Sti = Wds is shown by heavy dash-dotted line. The Anh-B + Sti = Rng boundary is insensitive to solid solution effects in both anhydrous and hydrous systems. The calculated net displacements of the stability limits of both Anh-B ± Sti in water-saturated natural system are shown by heavy dashed lines and arrows. The short light dashed lines indicate the likely expansion of the Anh-B + Sti field relative to Rng by lowering the Δ_fG of Anh-B by 5 kJ/mol, which is 0.04% of the estimated value; the corresponding expansion relative to Wads is almost the same as that shown by dash-dotted line. The thick grey lines with steep slopes indicate the P-T conditions of thermal minima in 140 Myr old slabs subducting at an angle of 60° with 14 and 8 cm/yr velocities, as calculated by *Bina and Navrotsky* [2000], using a plate model and basal lithospheric temperatures (BLT) of 1450°C and 1325°C.

icant expansion of the thermal stability limit of the assemblage Anh-B + Sti. By the same token raising the Δ_fG of Anh-B by the same amount would cause virtual disappearance of the stability field of Anh-B + Sti from the domain of P-T conditions attained within a subducting oceanic slab. Thus the results of our calculations are inconclusive about the stability of Anh-B + Sti, but should still be useful for guiding future experimental studies to investigate the stability of this assemblage.

5. Compositional Effects on the Stability of Anh-B

[22] In this section we explore the effects of solid solution on the equilibria (R1), (R2) and (R3). In addition to the usual cation substitutions, dissolution of H_2O in the nominally anhydrous minerals could also affect their stabilities [*Smyth*, 1987; *Wood*, 1995]. At this stage we do not have adequate data on element and H_2O fractionation, and thermodynamic mixing properties to calculate these dis-

placements. Nonetheless, we can develop a reasonable feeling for the likely direction and approximate magnitudes of the displacements of the equilibria in mantle compositions as follows.

[23] Following the suggestion of *Smyth* [1987] for the mechanism of dissolution of water in the different polymorphs of Mg_2SiO_4, *Wood* [1995] considered dissolution of H_2O in $(Mg, Fe)_2SiO_4$ in terms of solid solution between the end-member components $(Mg, Fe)_2SiO_{3.5}O_{0.5}$, which is equivalent to $(Mg, Fe)_2SiO_4$, and $(Mg, Fe)_{1.75}SiO_{3.5}(OH)_{0.5}$. (The solubility mechanism proposed by *Smyth* [1987] for wadsleyite has recently been confirmed by *Demouchy et al.* [2005].) Using the ionic solution model [e.g., *Ganguly and Saxena*, 1987], he thus expressed the activity of Mg_2SiO_4 as

$$a(Mg_2SiO_4) = \left[\left(X_{Mg}\gamma_{Mg} \right)^2 (1 - X_{OH})^{0.5} \right]_{Fo/Wads/Rng} \quad (6)$$

where X and γ stand for the atomic fraction and activity coefficient, respectively, of the specified ion in its structural site. It is assumed that the mixing within the individual structural sites is independent of one another.

[24] Following the logic of *Smyth* [1987], the O4 oxygen (nonsilicate oxygen) in Anh-B is a potential hydration site. Assuming that $(OH)^{-1}$ substitution is charge balanced by vacancy in divalent cation site, as in the case of hydration of olivine, the hydrated end-member of Anh-B should have a formula of $Mg_{13}Si_5O_{22}(OH)_2$. In that case, following *Wood*'s [1995] model for the activity Mg_2SiO_4 component (6), the activity of the anhydrous Mg end-member component of Anh-B may be expressed as

$$a(Mg_{14}Si_5O_{24}) = \left[\left(X_{Mg}\gamma_{Mg} \right)^{14} (X_{Si})^5 (1 - X_{OH})^2 \right]_{Anh-B}, \quad (7)$$

With the above activity expressions, the equilibrium constants of the reactions (R1), (R2) and (R3) become

$$K_{(R1)} = \frac{\left[\left(X_{Mg} \right)^{14} (X_{Si})^5 (1-X_{OH})^2 \right]_{Anh-B}}{\left[\left(X_{Mg} \right)^{10} \right]_{Ol} \left[\left(X_{Mg} \right)^4 \right]_{Per}} K_{\gamma(R1)} \quad (8a)$$

$$K_{(R2)} = \frac{\left[\left(X_{Mg} \right)^{14} \right]_{Ring}}{\left[\left(X_{Mg} \right)^{14} (X_{Si})^5 (1-X_{OH})^2 \right]_{Anh-B}} K_{\gamma(R2)} \quad (8b)$$

$$K_{(R3)} = \frac{\left[\left(X_{Mg} \right)^{14} \right]_{Wads}}{\left[\left(X_{Mg} \right)^{14} (X_{Si})^5 (1-X_{OH})^2 \right]_{Anh-B}} K_{\gamma(R3)} \quad (8c)$$

where K_γ stands for the collection of activity coefficient terms for each equilibrium. For brevity, we would designate the collection of compositional terms in the above expressions as $K_{X(R1)}$, $K_{X(R2)}$ and $K_{X(R3)}$, respectively.

[25] *Herzberg and Zhang* [1996] determined the compositions of coexisting Anh-B, olivine and garnet (Grt) that developed in KLB-1 peridotite composition at 15.5 GPa, 2100°C. On the other hand, *Frost* [2003] determined the

compositions of coexisting garnet and wadsleyite or ring-woodite at 14 GPa, 1400°C in the Ca-Fe-Mg-Al-Si-O system. We used these data sets to estimate the compositions of wadsleyite and ringwoodite that could have coexisted with the Anh-B compositions in KLB-1 bulk composition. It was assumed that X_{Mg}(Wads/Ring) varied linearly vs. X_{Mg}(Grt), satisfying the relation that at X_{Mg}(Wads/Rng) = 1, X_{Mg}(Grt) = 1. For anhydrous system, this exercise yields $K_{X(R1)}$ = 0.80, assuming $(X_{Mg})_{Per}$ = 1, $K_{X(R2)}$ = 1.02 and $K_{X(R3)}$ = 1.49. Since the compositions of the minerals are close to their respective pure end members, we assumed that $K_{\gamma(R1)} \approx K_{\gamma(R2)} \approx K_{\gamma(R3)} \approx 1$. The resultant displacements of pressure at 1400°C, as calculated according to standard thermodynamic procedure [e.g., *Ganguly and Saxena*, 1987, equation 4.27), and assuming $\Delta_r V$ to be constant, are -0.3 GPa for (R1), 0.1 GPa for (R2) and -1.4 GPa for (R3), the negative signs indicating displacements toward lower pressure. The magnitude of displacement of the equilibrium (R1) should be even smaller since $(X_{Mg})_{Per}$ should be somewhat less than unity, thus raising the $K_{X(R1)}$ value.

[26] An obvious drawback with the above calculations is our implicit assumption that the element fractionations are insensitive to changing P-T conditions since we have combined data from different P-T conditions (14 GPa, 1400°C and 15.5 GPa, 2100°C) to calculate the K_X values. Nonetheless, these calculations suggest that the solid solution effects on the displacements of the equilibria defining the stability of Anh-B should be quite small in an anhydrous natural system. Assuming that the displacements of the equilibria due to compositional effects are approximately parallel to their Mg end-member boundaries in the P-T space, we have illustrated the compositional shift of the equilibrium (R3) by a dash-dotted line in Figure 3.

[27] Using the data on the maximum water solubility in olivine by *Kohlstedt et al.* [1996] and reinterpreting their spectroscopic data, *Hirschmann et al.* [2005] suggested that the H_2O storage capacity of olivine at the greatest depths of its stability is $\sim$5000 ppm. Recently, J. Smyth and D. J. Frost (unpublished data, 2005) synthesized olivines with up to 8500 ppm H_2O. J. Smyth (personal communication, 2005) estimated that if olivine has a maximum of 8500 ppm H_2O, then the maximum of H_2O contents of wadsleyite should be $\sim$33,000 ppm, that of ringwoodite $\sim$22,000 ppm and of Anh-B $\sim$21,000 ppm. The estimate for wadsleyite is consistent with that made by *Hirschmann et al.* [2005] from a critical analysis of the available experimental data on H_2O solubility in this mineral. *Demouchy et al.* [2005] determined the water solubility in wadsleyite as function of pressure and temperature. They did not observe any significant effect of pressure on the water solubility in wadsleyite, but found that at a pressure of 15 GPa, the water solubility decreased from 22,000 ppm at 900°C to 9000 ppm at 1400°C.

[28] For the purpose of present calculation, we assume that the equilibrium partitioning of H_2O between two phases may be approximated by the ratio of the respective water solubility limits. This procedure yields $(H_2O)_{Wads}/(H_2O)_{Rng}$ = 3.8, which is similar to that (5 ± 0.3) reported by *Chen et al.* [2002] from experimental studies. Thus, using the above estimates of maximum water solubilities and equilibrium cation fractionations, we obtain $K_{X(R1)}$ = 0.4, $K_{X(R2)}$ = 1.1

and $K_{X(R3)}$ = 0.5 leading to shifts of the equilibrium boundaries of -1 GPa for (R1), 0.4 GPa for (R2) and 2.6 GPa for (R3) at 1400°C. These shifts of the equilibrium boundaries are illustrated in Figure 3 as bold dashed lines and arrows, assuming that these are not significantly affected by temperature changes.

[29] From the above calculations, it seems that the equilibrium boundary between Anh-B + St and ringwoodite is insensitive to compositional changes under both anhydrous and hydrous conditions, whereas the stability of Anh-B + St with respect to wadsleyite could be slightly expanded under anhydrous condition or significantly depressed under water saturated condition. The equilibrium boundary between Anh-B with respect to Fo + Per can be lowered in pressure by a maximum of $\sim$1 GPa by combination of the effects of hydroxyl and cation substitutions.

6. Geophysical Implications

[30] In order to evaluate if the assemblage Anh-B + Sti could become stable within cold slabs, we have superimposed (Figure 3) the approximate range of P-T conditions that are likely to be encompassed by the thermal minima within cold slabs on the calculated stability field of Anh-B + Sti. The thermal profiles are taken from *Bina and Navrotsky* [2000], who used subduction angle of 60°, slab age of 140 Myr, and subduction velocity (v) of 8 cm/yr or 14 cm/yr. The parameters for the slower and faster dipping plates are similar to those of the Indonesian and Tonga plates, respectively. Using plate model, *Bina and Navrotsky* [2000] computed two thermal profiles for each set of conditions, one with a relatively high basal lithospheric temperature (BLT) of 1450°C [*Stein and Stein*, 1992] and other with a lower BLT of 1325°C [*Davies and Stevenson*, 1992].

[31] We show in Figure 3 the profiles of thermal minima for BLT of 1450°C and both 8 and 14 cm/yr subduction velocities, as well as that of thermal minimum with BLT of 1325°C and 14 cm/yr subduction velocity. According to the calculation of *Bina and Navrotsky* [2000], the change of the model from plate to half-space would cause around $40°-50°$C reduction of temperature of the thermal minimum at $10-20$ GPa. Both shear and radiogenic heating were ignored in these model calculations, but the effect of these parameters on the thermal minima shown in Figure 3 would likely be more than compensated by the change from plate and half-space model and other effects, as discussed by *Bina and Navrotsky* [2000]. In addition, these authors also noted that the subduction velocity can be much higher, up to 24 cm/yr, in north Tonga thereby causing significant depression of temperature below that shown by the 14 cm/yr profile in Figure 3.

[32] The comparison of thermal minima of cold slabs and the phase relations (Figure 3) suggests the possibility of the reaction sequence Wads → Anh-B + St → Rng, instead of the direct transformation of wadsleyite to ringwoodite, within some cold oceanic slabs. The 410 km global seismic discontinuity in the mantle is generally believed to be due to the transformation of wadsleyite to ringwoodite. The formation of Anh-B + Sti would, in principle, cause an eye-shaped splitting of this discontinuity within the interior of a cold slab.

[33] A number of recent seismic studies in different parts of the world in a range of subcontinental and subduction

zone environments have revealed seismic discontinuity at 275–345 km depth [e.g., *Revenaugh and Jordan*, 1991; *Revenaugh and Williams*, 2000; *Owens et al.*, 2000; *Gilbert et al.*, 2003]. This has been called X discontinuity by *Revenaugh and Jordan* [1991]. This discontinuity is a subtle feature reflecting only about 2–3% of incident SH energy consistent with 4–6% increase in shear wave impedance [*Revenaugh and Williams*, 2000]. The density change associated with this discontinuity has not yet been constrained. The nature of mineralogical transition(s) causing this discontinuity still remains an unsolved problem. *Woodland* [1998] suggested the orthorhombic to monoclinic transition of ferromagnesian pyroxenes as a possible cause of this discontinuity. *Revenaugh and Williams* [2000] argued against this suggestion since the "anticipated impedance increase" is too small and "the reaction is intrinsically limited to mantle wedge." They suggested the coesite to stishovite transition as the likely cause of the X discontinuity. The silica was envisioned to have been precipitated from water given off by subducting slabs at depths greater than 300 km. *Williams and Revenaugh* [2000] suggested that pervasive veining of silica would prevent it from completely reacting with the surrounding olivine in the mantle to form orthopyroxene.

[34] We have compared in Figure 3 the coesite-stishovite transition boundary [*Saxena et al.*, 1993] with that between Fo + Per and Anh-B. It is interesting to note that from the standpoint of phase relations, both equilibria are equally capable of explaining the X discontinuity. However, as opposed to the coesite-stishovite transition that requires local enrichment of silica, the formation of Anh-B requires local enrichment of MgO.

[35] It is conceivable that water plays the role of redistribution of silica by dissolving the silica out of olivine and orthopyroxene according to $(Mg, Fe)_2SiO_4 = 2 (Mg, Fe)O + SiO_2(aq)$ and $(Mg, Fe)SiO_3 = (Mg, Fe)O + SiO_2(aq)$, where $SiO_2(aq)$ implies silica dissolved in the aqueous phase, and precipitating silica elsewhere. The redistribution of silica would lead to two transitions at essentially the same depth, Fo + Per to Anh-B and coesite to stishovite. In this scenario, water is not presaturated with silica as it comes in contact with mantle minerals, and need not be completely derived from the subducting slab. Indeed, a subducting slab younger than 50 Ma would be essentially dehydrated when it subducts to a depth of ~200 km [*Bose and Ganguly*, 1995]. Thus, if silica precipitation from a slab derived fluid and the consequent coesite to stishovite transition were the sole reason for the X discontinuity, then it should not be observed in areas that are associated with slabs younger than 50 Ma, and those that are not associated with active or extinct subduction zone environment, such as reported by *Owens et al.* [2000].

[36] *Stalder et al.* [2001] determined the compositions of supercritical fluid and melt formed by the hydrous melting in the model mantle system MgO-SiO_2-H_2O at 6–10 GPa, 900–1200°C. They found that the hydrous eutectic melting between forsterite and enstatite gives way to incongruent melting of forsterite between 6 and 8 GPa. Thus, if there is hydrous melting of the mantle above this pressure, such as suggested by *Huang et al.* [2005], then it would lead to the formation of a melt that is somewhat richer in MgO than the surrounding mantle. This melt could also be a likely source of MgO that is needed for the formation of anhydrous B by reaction with forsterite.

[37] Whether the process of pervasive veining of the mantle can protect the silica from reacting with olivine to form orthopyroxene, as suggested by *Williams and Revenaugh* [2000], depends on the kinetics of chemical communication between forsterite and silica across an intermediate layer of orthopyroxene that had already formed by the reaction between Fo and SiO_2. We can gain an approximate idea of the extent of this chemical communication as a function of time by considering diffusive transport of Mg. For this purpose, we take the volume diffusion of Mg in olivine as a lower bound to the kinetics of diffusive transport Mg. Using the data from *Chakraborty et al.* [1994] and *Chakraborty* [1997] on Fe-Mg interdiffusion coefficient in olivine as a function of P and T up to 10 GPa and 1350°C yields effective diffusion distance (x), as calculated from the Einstein relation of $x = (2Dt)^{1/2}$, of ~10 cm in 10 My. This probably represents a conservative estimate of x since the intergranular transport in the presence of H_2O could be significantly faster than volume diffusion. (Note that under dry condition, volume diffusion should be faster than intergranular diffusion at high temperature such as at 300 km depth in the mantle [e.g., *Shewmon*, 1963; *Ganguly*, 2002].) Because of the square root dependence of x on t, this distance would change by a factor 1.4 as t changes by a factor of 2. It remains to be seen if there could be enough silica veining in the mantle to yield significant amount of residual silica after forming a protective orthopyroxene layer that has a thickness in excess of the effective diffusion distance of Mg.

References

Bina, C. R., and A. Navrotsky (2000), Possible presence of high-pressure ice in cold subducting slabs, *Nature*, *408*, 844–847.

Bose, K., and J. Ganguly (1995), Experimental and theoretical studies of the stabilities of talc, antigorite and phase A at high pressure with applications to subduction processes, *Earth Planet. Sci. Lett.*, *136*, 109–121.

Chakraborty, S. (1997), Rates and mechanisms of Fe-Mg interdiffusion in olivine at 980°–1300°C, *J. Geophys. Res.*, *102*, 12,317–12,331.

Chakraborty, S., J. R. Farver, R. A. Yund, and D. C. Rubie (1994), Mg tracer diffusion in synthetic forsterite and San Carlos olivine as a function of P, T and fO$_2$, *Contrib. Mineral. Petrol.*, *21*, 489–500.

Chen, J., T. Inoue, H. Yurimoto, and D. J. Weidner (2002), Effect of water on olivine-wadsleyite phase boundary in the (Mg, Fe)$_2$SiO$_4$ system, *Geophys. Res. Lett.*, *29*(18), 1875, doi:10.1029/2001GL014429.

Chermak, J. A., and J. D. Rimstidt (1989), Estimating the thermochemical properties of (ΔG_f^o and ΔH_f^o) of silicate minerals at 298 K from the sum of polyhedral contributions, *Am. Mineral.*, *74*, 1023–1031.

Davies, J. H., and D. J. Stevenson (1992), Physical model of source region of subduction zone volcanics, *J. Geophys. Res.*, *97*, 2037–2070.

Demouchy, S., E. Deloule, D. J. Frost, and H. Keppler (2005), Pressure and temperature-dependence of water solubility in Fe-free wadsleyite, *Am. Mineral.*, *90*, 1084–1091.

Fabrichnaya, O. B., S. K. Saxena, P. Richet, and E. F. Westrum (2004), *Thermodynamic Data, Models and Phase Diagrams in Multicomponent Oxide Systems*, Springer, New York.

Finger, L. M., R. M. Hazen, and C. T. Prewitt (1991), Crystal structures of $Mg_{12}Si_4O_{19}(OH)_2$ (phase B) and $Mg_{14}Si_5O_{24}$ (phase AnhB), *Am. Mineral.*, *76*, 1–7.

Frost, D. J. (2003), Fe^{2+}-Mg partitioning between garnet, magnesiowüstite and $(Mg,Fe)_2SiO_4$ phases of the transition zone, *Am. Mineral.*, *88*, 387–397.

Fyfe, W. S., F. J. Turner, and J. Verhoogen (1958), Metamorphic Reactions and Metamorphic Facies, *Mem. Geol. Soc.*, *73*.

Ganguly, J. (2002), Diffusion kinetics in minerals: Principles and applications to tectono-metamorphic processes, in *Energy Modelling in Minerals*, *EMU Notes Mineral.*, vol. 4, pp. 271–309, Eötvös Univ. Press, Budapest.

Ganguly, J., and S. K. Saxena (1987), *Mixtures and Mineral Reactions*, Springer, New York.

Gilbert, H. J., A. F. Sheehan, K. G. Dueker, and P. Molnar (2003), Receiver functions in the western United States, with implications for upper mantle structure and dynamics, *J. Geophys. Res.*, *108*(B5), 2229, doi:10.1029/2001JB001194.

Herzberg, C. H., and T. Gasparik (1989), Melting experiments on chondrite at high pressures: Stability of anhydrous B, *Eos Trans. AGU*, *70*(16), 484.

Herzberg, C. H., and J. Zhang (1996), Melting experiments on anhydrous peridotie KLB-1: Compositions of magma in the upper mantle and transition zone, *J. Geophys. Res.*, *101*, 8271–8295.

Hirschmann, M. M., C. Aubaud, and A. C. Withers (2005), Storage capacity of H_2O in nominally anhydrous minerals in the upper mantle, *Earth Planet Sci Let.*, *236*, 181–267.

Holland, T. J. B. (1989), Dependence of entropy on volume for silicate and oxide minerals: A review and predictive model, *Am. Mineral.*, *74*, 5–13.

Huang, X., Y. Xu, and S.-I. Karato (2005), Water in the transition zone from electrical conductivity of wadseleyite and ringwoodite, *Nature*, *434*, 746–749.

Kato, T., and M. Kumazawa (1985), Stability of phase B, a hydrous magnesium silicate, to 2300°C at 23 GPA, *Geophys. Res. Lett.*, *12*, 534–535.

Keppler, H., and D. J. Frost (2005), Introduction to minerals under extreme conditions, in *Mineral Behaviour at Extreme Conditions*, *EMU Notes Mineral.*, vol. 7, edited by R. Miletich, Eötvös Univ. Press, Budapest, in press.

Kohlstedt, D., H. Keppler, and D. C. Rubie (1996), Solubility of water in the α, β and γ phases of $(Mg, Fe)_2SiO_4$, *Contrib. Mineral. Petrol.*, *123*, 345–357.

Owens, T. J., A. A. Nyblade, H. Gurrola, and C. A. Langston (2000), Mantle transition zone structure beneath Tanzania, East Africa, *Geophys. Res. Lett.*, *27*, 827–830.

Revenaugh, J., and T. H. Jordan (1991), Mantle layering from ScS reverberations: 3. The upper mantle, *J. Geophys. Res.*, *96*, 19,781–19,810.

Revenaugh, J., and Q. Williams (2000), The seismic X discontinuity: Observations and modeling, *Eos Trans. AGU*, *81*(48), Fall Meet. Suppl., Abstract S21E-05.

Saxena, S. K. (1996), Earth mineralogical model: Gibbs free energy minimization computation in the system $MgO-FeO-SiO_2$, *Geochim. Cosmochim. Acta*, *60*, 2379–2395.

Saxena, S. K., N. Chatterjee, Y. Fei, and G. Shen (1993), *Thermodynamic Data on Oxides and Silicates*, Springer, New York.

Shewmon, P. G. (1963), *Diffusion in Solids*, McGraw-Hill, New York.

Smyth, J. R. (1987), β-Mg_2SiO_4: A potential host for water in the mantle?, *Am. Mineral.*, *72*, 1051–1055.

Stalder, R., P. Ulmer, A. B. Thompson, and D. Günther (2001), High pressure fluids in the system $MgO-SiO_2-H_2O$ under upper mantle conditions, *Contrib. Mineral. Petrol.*, *140*, 607–618.

Stein, C. A., and S. A. Stein (1992), A model for the global variation of oceanic depth and heat flow with lithospheric age, *Nature*, *359*, 123–129.

Williams, Q., and J. S. Revenaugh (2000), The X-discontinuity: A signature of deep fluid flow and free silica in the sub-continental mantle, *Eos Trans. AGU*, *81*(48), Fall Meet. Suppl., Abstract S21E-07.

Wood, B. J. (1995), The effect of H_2O on the 410-kilometer seismic discontinuity, *Science*, *268*, 74–76.

Woodland, A. B. (1998), The orthorhombic to high-P monoclinic phase transition in Mg-Fe pyroxene: Can it produce a seismic discontinuity?, *Geophys. Res. Lett.*, *25*, 1241–1244.

———————————

D. J. Frost, Bayerisches Geoinstitut, Universität Bayreuth, Bayreuth, D-94550, Germany.

J. Ganguly, Department of Geosciences, University of Arizona, 1040 E. Fourth Street, Tucson, AZ 85721, USA. (ganguly@geo.arizona.edu)